https://doi.org/10.5194/egusphere-2026-1556
Preprint. Discussion started: 5 June 2026

Seasonal Predictability of Antarctic Sea Ice based on a Deep-learning Approach

Gyeongmin Baek[1], Jiho Ko[2], Emilia Kyung Jin[3], Jong-Seong Kug[1,2]

[1]School of Earth and Environmental Sciences, Seoul National University, Seoul, 08826, South Korea
[2]Interdisciplinary Program in Artificial Intelligence, Seoul National University, Seoul, 08826, South Korea
[3]Korea Polar Research Institute, Incheon, 21990, South Korea

Correspondence to: Jong-Seong Kug (jskug@snu.ac.kr)

Abstract. Arctic sea ice has steadily declined under global warming, whereas Antarctic sea ice, after a modest multi-decadal increase, began a sharp downturn in 2016 and reached a record minimum in February 2023. These recent changes highlight the need for improved seasonal prediction of Antarctic sea-ice variability, particularly during austral summer when conventional numerical models often have limited skill. Here, we develop a deep-learning framework for seasonal prediction of Antarctic sea ice using a selective set of physically relevant atmospheric and oceanic predictors. The model substantially improves predictability in austral summer while maintaining a physically interpretable representation of the underlying drivers. To go beyond prediction skill alone, we examine the model using spatially explicit and seasonally resolved explainable artificial intelligence contribution maps. These reveal distinct seasonal predictor influences: meridional wind (V) dominates in austral summer (Dec–Feb), whereas downward shortwave radiation (SW) is most important in austral spring (Sep–Nov). The influence of V on sea ice differs between summer and winter, while springtime SW contributions show marked regional contrasts, suggesting that the model captures cloud-mediated feedbacks. Together, these results demonstrate that deep learning can not only improve seasonal Antarctic sea-ice forecasts but also provide physically interpretable insights into atmosphere–ocean–sea-ice interactions across space and time.

1 Introduction

Unlike the persistent declining trend observed in Arctic sea ice, Antarctic sea ice previously exhibited a modest increasing trend (Comiso et al., 2017; Parkinson and Cavalieri, 2012). Notably, between 2013 and 2015, sea ice concentration (SIC) remained above the climatological average; however, beginning in 2016, it underwent a sharp decline that has persisted with record-low extents thereafter (Fogt et al., 2022; Zhang et al., 2022). Numerous studies have discussed the causes of this recent Antarctic sea ice reduction, attributing the abrupt decline in 2016 primarily to increased sea surface temperatures (SST), while linking the record-low conditions in 2023 to altered meridional heat fluxes (Purich and Doddridge, 2023). More recently, attention has focused on the role of subsurface ocean heat (Purich and Doddridge, 2023), highlighting growing

https://doi.org/10.5194/egusphere-2026-1556
Preprint. Discussion started: 5 June 2026

scientific interest in the underlying mechanisms. This decline arises from multiple contributing factors, underscoring the need for deeper investigation.

Antarctic sea ice plays a crucial role in the global climate system. It acts as a buffer, mitigating sea-level rise by preventing rapid discharge of meltwater from ice sheets into the ocean (Massom et al., 2018). Sea ice loss freshens the surface layer and enhances ocean stratification (Lucas et al., 2025). This process inhibits heat exchange within the Southern Ocean, thereby reducing the ocean's capacity for carbon sequestration and adversely affecting marine ecosystems (Li et al., 2020; Venegas et al., 2023). Furthermore, the high albedo of sea ice effectively reflects solar radiation, playing a crucial role in regulating polar temperatures (Cai et al., 2021; Curry et al., 1995). In addition, diminishing sea ice disrupts logistical routes used to transport supplies to Antarctic research stations, potentially resulting in significant economic losses (Doddridge et al., 2025).

Given this context, accurately predicting Antarctic sea ice variability is crucial for understanding global climate systems and mitigating potential economic impacts. However, Antarctic sea ice remains difficult to predict at seasonal time scales, and both statistical and dynamical forecasting approaches often show limited skill and strong regional dependence (Chen and Yuan, 2004; Hogg et al., 2020; Morioka et al., 2019; Zampieri et al., 2019). Current forecasting efforts, including those of the Sea Ice Prediction Network South (SIPN South), still exhibit limited skill, and the low reliability of individual models raises concerns about their practical applicability. As a result, the current level of predictive accuracy remains inadequate to effectively support scientific research and logistical planning for polar navigation (Massonnet et al., 2023). For instance, Bushuk et al. (2021) demonstrated that Antarctic sea ice predictions using the GFDL dynamical model showed skillful forecasts up to 11 months in advance for most regions during winter, but notably lower skill in the Ross Sea region. Additionally, summer predictions are generally less reliable than winter forecasts because of more complex influencing factors, with performance particularly low in October when rapid sea ice loss takes place.

Recently, deep learning has been increasingly adopted for Antarctic sea-ice prediction. Wang et al. (2023) demonstrated skillful subseasonal forecasts at lead times of 1–4 weeks using sea-ice information alone. Extending prediction beyond subseasonal time scales, however, likely requires accounting for atmospheric forcing and oceanic memory that shape sea-ice evolution over months. In this context, Yang et al. (2025) advanced seasonal prediction by introducing a U-Net–based framework (ANTSIC-UNet) that integrates additional atmospheric and oceanic predictors to represent coupled processes governing Antarctic sea-ice variability. Building on these advances, we develop a multi-variable deep learning framework for seasonal prediction of Antarctic sea ice extent. To improve model efficiency while retaining physical relevance, we employ a selective set of key input variables rather than a broad collection of predictors, focusing the learning process on the most influential drivers of Antarctic sea-ice variability. Importantly, our study goes beyond prediction skill by examining the model's behavior using explainable artificial intelligence (XAI). Through spatially and seasonally resolved contribution maps, we investigate where, when, and which predictors most strongly influence the forecasts across Antarctic regions, and we use these patterns to derive physically meaningful interpretations of the drivers of sea-ice variability.

https://doi.org/10.5194/egusphere-2026-1556
Preprint. Discussion started: 5 June 2026

2 Data and Methods

2.1 Data

Monthly data from 1979 to 2023 were used to train and validate the deep learning model. However, this provides a relatively limited sample size for deep learning, which constrains model training if observations alone are used. To overcome the limitations of observations and improve model generalization as well as the representation of internal variability, different datasets were utilized during the pre-training and fine-tuning phases. In the pre-training stage, the model was trained on the Community Earth System Model version 2 Large Ensemble (LENS2), which comprises a 160-year historical simulation with 10 ensemble members (Danabasoglu et al., 2020; Rodgers et al., 2021). Although LENS2 data show differences in climatological mean state and long-term trends relative to observations (Fig. S1), they sufficiently represent dynamic processes associated with seasonal sea ice changes. To assess whether these mean-state differences affect model training, we conducted an experiment using two datasets: the full LENS2 period and only the last 40 years, during which the climatological baseline is most similar to observations. The results from the two experiments were nearly identical, indicating that the mean-state differences in LENS2 did not produce a meaningful difference in the training outcome.

The input variables include sea ice concentration (SIC), downward shortwave radiation (SW, all referring to downward flux), zonal wind at 10 m (U), meridional wind at 10 m (V), sea level pressure (SLP), sea surface temperature (SST), and ocean potential temperature at 200 m depth (PT) —to represent the dominant sources of seasonal predictability for Antarctic sea ice while maintaining physical interpretability and consistency across training datasets. The chosen predictors are intended to capture three complementary pathways that govern seasonal sea-ice evolution: (i) sea-ice persistence, (ii) fast atmospheric forcing through surface energy fluxes and dynamics, and (iii) slowly varying oceanic thermal conditions that provide longer-lived boundary forcing. Variables such as cloud fraction, longwave radiation, and salinity can also affect Antarctic sea ice, but were not included in the baseline configuration due to constraints related to cross-dataset consistency, uncertainty in high-latitude retrievals/reanalyses, and the desire to keep the model interpretable. We therefore treat the omission of these variables as a limitation and identify their inclusion and direct comparison as an important direction for future work.

In the fine-tuning phase, reanalysis datasets were employed depending on the specific variables: SIC was obtained from NSIDC's Nimbus-7 SMMR and DMSP SSM/I-SSMIS Passive Microwave Data, Version 2 (DiGirolamo et al., 2022); atmospheric variables (SW, U, V, and SLP) were sourced from the NCEP2 Reanalysis (Kanamitsu et al., 2002); SST was taken from ERSSTv5 (Huang et al., 2017); and PT was acquired from ORAS5 reanalysis data (Copernicus Climate Change Service and Climate Data Store, 2021). The fine-tuning input data spanned 44 years of observations, from 1980 to 2023.

The model output was defined as area-mean sea ice extent anomalies for five Antarctic regions: Weddell, Indian, West Pacific (WP), Ross, and Amundsen-Bellingshausen (AB, Fig. 1). Predicting regional mean sea ice extent enables the model to capture large-scale sectoral variability, facilitating consistent interpretation across predefined regions. To ensure consistency across variables, all input data were interpolated onto a uniform 1° × 1° grid, covering latitudes from 49.5°S to

https://doi.org/10.5194/egusphere-2026-1556
Preprint. Discussion started: 5 June 2026

89.5°S and longitudes from 0° to 360°. Seasonal means were then subtracted to compute anomalies, and all input variables were normalized. To account for grid size distortion at higher latitudes, latitude-based weighting was applied in the calculation of sea ice extent. The performance of the deep learning model was benchmarked against numerical forecast models from Copernicus Climate Change, including ECMWF, DWD, Met Office, and Météo-France (Copernicus Climate Change Service and Climate Data Store, 2018).

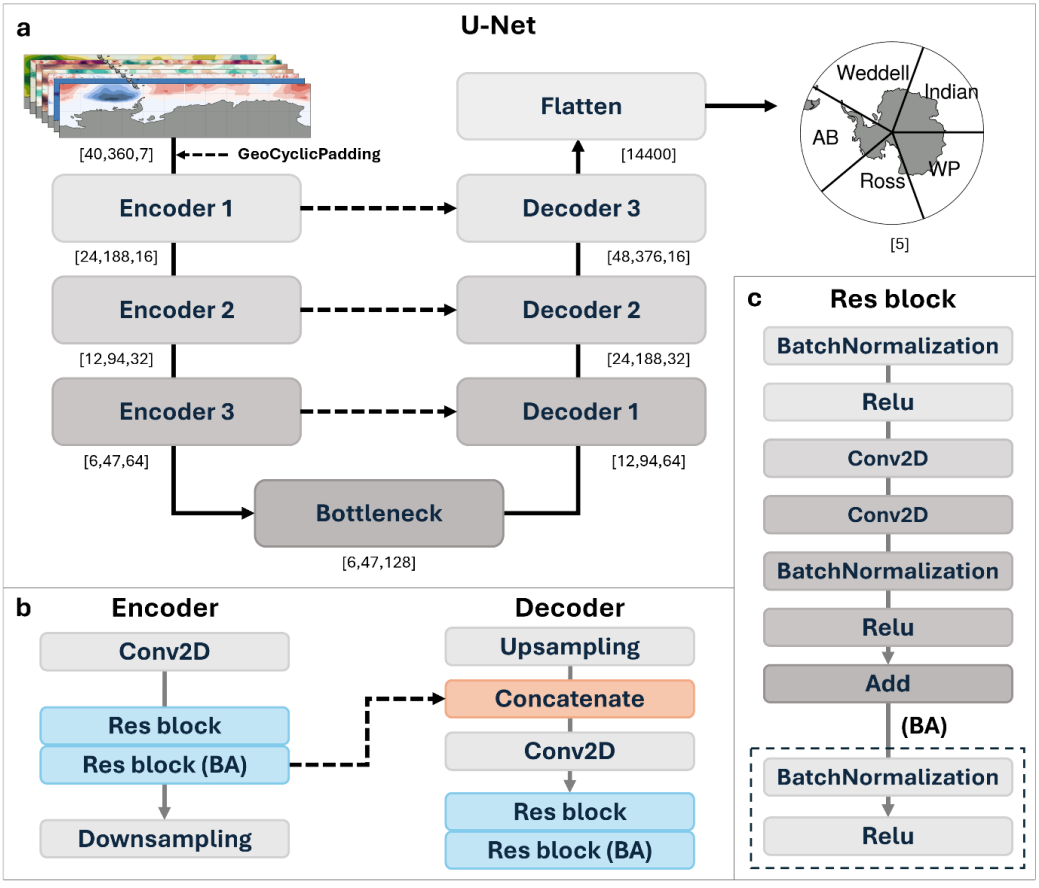

Figure 1: U-Net model architecture and the five Antarctic regions defined by longitude (Weddell, Indian, West Pacific, Ross, Amundsen-Bellingshausen). (a) U-Net architecture. **(b)** Encoder and decoder structures. The encoder's residual block (BA) is connected to the corresponding upsampled feature map in the decoder through skip connections. BA (BatchActivation) consists of a Batch Normalization followed by ReLU. **(c)** Structure of the residual block. After passing through Batch Normalization and ReLU, the input is processed by two Conv2D layers. Following the second Conv2D, another Batch Normalization and ReLU are applied. The result is then added to the block's input. In the case of the Res block (BA), an additional Batch Normalization and ReLU are applied afterward.

2.2 U-Net and Transfer Learning

A U-Net-based deep learning model (Ronneberger et al., 2015) incorporating residual connections was developed for simultaneous prediction of sea ice extent across the five Antarctic regions. Model inputs consist of tensors with dimensions

https://doi.org/10.5194/egusphere-2026-1556
Preprint. Discussion started: 5 June 2026

(Latitude, Longitude, Channel), where Latitude and Longitude denote spatial resolution, and Channel indicates the number of geophysical input variables. Outputs comprise scalar predictions for each of the five regions.

The encoder includes convolutional blocks, residual blocks, and downsampling (max-pooling). Dilated convolutions (Yu and Koltun, 2016) with a dilation rate of 2 were employed at the bottleneck for an expanded receptive field. The decoder mirrors the encoder structure, integrating encoder features through skip connections and employing residual blocks to ensure training stability. Each residual block consists of two convolutional layers, Batch Normalization (Ioffe and Szegedy, 2015), ReLU activation functions (Nair and Hinton, 2010), and shortcut connections (Fig. 1).

GeoCyclicPadding (Cheon et al., 2024) was introduced to mitigate boundary discontinuities associated with traditional zero-padding by cyclically extending values in latitude and longitude. The padded inputs were fed into a U-Net with an encoder-decoder structure and restored to their original dimensions by GeoCyclicUnpadding after the final convolutional layer.

L2 regularization ($\lambda = 0.01$) (Barnes et al., 2020) was applied to all convolutional and dense layers, and Dropout was incorporated during downsampling and upsampling to prevent overfitting. The final decoder feature map was flattened and passed through independent fully connected branches for each region, each containing four hidden layers (256, 128, 64, and 32 neurons) with ReLU activation and a linear output layer. Convolutional layers were initialized with the He normal distribution (He et al., 2015).

Training consists of pre-training and fine-tuning phases. Pre-training utilized LENS2 data with the Adam optimizer and a cosine decay schedule, reducing learning rates from 0.01 to 0.0001. Mean Absolute Error (MAE) was used as the loss function, with early stopping applied based on validation loss, up to a maximum of 500 epochs with batch size 32. Fine-tuning employed observational and reanalysis datasets, starting with a learning rate of 0.00001 and a batch size of 16. To retain general representations and minimize overfitting, all layers except the final six were frozen.

During the pre-training, the data were divided based on ensemble members. Out of 10 ensemble members, 8 were used for the training, 1 was used as the validation set, and the remaining 1 was used as the test set. For the fine-tuning, we applied K-fold cross-validation by splitting the data into 11 subsets. In each round, 10 subsets were used for training and 1 subset was used for testing. This process was repeated 11 times, resulting in sea ice extent predictions for a total of 44 years.

2.3 Contribution map

To quantify the relative contribution of input variables to sea ice predictions, we employed the Contribution map method proposed by Shin et al. (2022), which is based on the occlusion sensitivity approach (Zeiler and Fergus, 2014). This method generates two predictions: one using the original, unchanged input variables, and another with specific grid values set to zero to eliminate their anomalous effects. The difference between these two predictions is measured using the Root-Mean-Squared Difference (RMSD), representing each grid's contribution. Additionally, region-specific average RMSDs were computed for each of the five Antarctic regions.

https://doi.org/10.5194/egusphere-2026-1556
Preprint. Discussion started: 5 June 2026

$$D_i^{j,k} = f(X_i) - f(X_i^{j,k}) \quad (1)$$

In this method, the function f represents the U-Net model, X_i refers to the input data for the i^{th} sample, and $X_i^{j,k}$ represents the array where the value of the j^{th} input variable at the k^{th} spatial grid location has been replaced with its climatological zero value. Therefore, $f(X_i)$ is the U-Net prediction with no alterations, and $f(X_i^{j,k})$ is the prediction with the j^{th} input variable at the k^{th} grid location zeroed out. The difference between these two predictions ($D_i^{j,k}$) signifies the contribution of the j^{th} input variable and k^{th} grid.

$$RMSD^{j,k} = \sqrt{\overline{D_i^{j,k^2}}} \quad (2)$$

Here, the Root Mean Square Difference (RMSD), calculated as the root mean square of $D_i^{j,k}$ across all samples, measures the importance of each variable over the period, highlighting variables significantly influencing the predicted sea ice extent.

2.4 Signed-contribution map

The RMSD is a metric that merely indicates the magnitude of changes in model predictions for given variables and grid points, without distinguishing whether these variables act to increase or decrease sea ice extent. Therefore, we employed a Signed-Contribution (SC) map (Shin et al., 2024) to assess not only the magnitude but also the direction of each variable's contribution to the predicted values.

$$D_i^{j,k^{high}} = \overline{D_i^{j,k}}^{X(j,k)_i > SD_{j,k}}; D_i^{j,k^{low}} = \overline{D_i^{j,k}}^{X(j,k)_i < -SD_{j,k}} \quad (3)$$

Here, $X(j,k)_i$ denotes the value of the i^{th} sample for the j^{th} input variable at the kth grid location, and $SD_{j,k}$ represents 0.1 times the standard deviation of $X(j,k)$. The SC map is derived by first calculating the difference $D_i^{j,k}$ between the predictions made by perturbing each input variable at each grid point and the original predictions. Subsequently, the SC value for each input variable at each grid point is computed by subtracting the average of $D_i^{j,k}$ values smaller than $-SD_{j,k}$ from the average of those greater than $SD_{j,k}$.

$$SC^{j,k} = D_i^{j,k^{high}} - D_i^{j,k^{low}} \quad (4)$$

Unlike the contribution map derived solely from RMSD, which provides only the magnitude of contributions without directional information, the SC map enables a clear understanding of both the intensity and direction (positive or negative) of each input variable's contribution at every grid point.

https://doi.org/10.5194/egusphere-2026-1556
Preprint. Discussion started: 5 June 2026

2.5 Skill metrics

To quantitatively evaluate the predictive performance of the model, the Anomaly Correlation Coefficient (ACC) and Root-Mean-Squared Error (RMSE) were utilized. Both metrics are widely used indicators for assessing the accuracy and reliability of predictive models, and they were employed in this study to objectively assess model performance. These two metrics comprehensively evaluate the model's capability to capture seasonal-scale sea ice variability, thereby providing critical insights into the predictive performance of the U-Net model and enabling meaningful comparative evaluations with numerical models.

3 Results

3.1 Performance of U-Net

Before applying fine-tuning with observations, we evaluated the performance of the U-Net model, pre-trained solely on LENS2. When assessed comprehensively across all seasons (Fig. S2), the U-Net model demonstrated superior ACC and RMSE compared to numerical models without fine-tuning. In the time series analysis, the pre-trained model reasonably captures the overall trends, although an overestimation is observed from the mid-1990s to the early 2000s (Fig. S2). Despite no training with observational data, the model exhibits high predictive skill. However, a noticeable bias during the austral winter (JJA) prompts additional fine-tuning using observational data. To correct the bias observed in the pre-trained model, transfer learning was conducted using reanalysis and observational data.

After the fine-tuning with observations, the U-Net model shows an ACC of 0.69 (Fig. 2a) and RMSE of 0.0094 (Fig. 2b) for all seasons. By comparison, the high-performing numerical models such as DWD and ECMWF show slightly lower ACC values of 0.65 and 0.61 and higher RMSE values of 0.0123 and 0.0122, respectively, with the lowest-performing numerical model recording an ACC of 0.29 and RMSE of 0.0342. In addition, the U-Net model shows superior performance in each season, maintaining more stable and consistent predictions of sea ice variability than the numerical models despite the seasonal dependence of the predictive skill. Both numerical models and U-Net exhibit their highest performance in autumn (MAM), with U-Net outperforming numerical models. In spring (SON), numerical models have ACC values below 0.3, while the U-Net shows ACC values above 0.6 (Fig. 2d). The tendency toward overestimation observed during pre-training is improved through fine-tuning, resulting in predictions closer to the observations (Fig. 2k,l,m,n,o). In particular, winter biases are reduced, indicating improved accuracy. Numerical models typically underestimate sea ice before 2006 and subsequently overestimate it afterward (Fig. 2k). In contrast, the U-Net model consistently performs better in terms of ACC and RMSE throughout the entire period (Fig. 2a,f). Moreover, the recent decreasing trend in Antarctic sea ice after 2016, following a prolonged period of increase, is reasonably captured by U-Net, aligning closely with the observational data. However, during the period of abrupt Antarctic sea ice decline in austral spring 2016, the U-Net model fails to clearly capture the extent of the

https://doi.org/10.5194/egusphere-2026-1556
Preprint. Discussion started: 5 June 2026

decrease (Fig. 2n). Similarly, most numerical models struggle to predict this extreme reduction accurately.

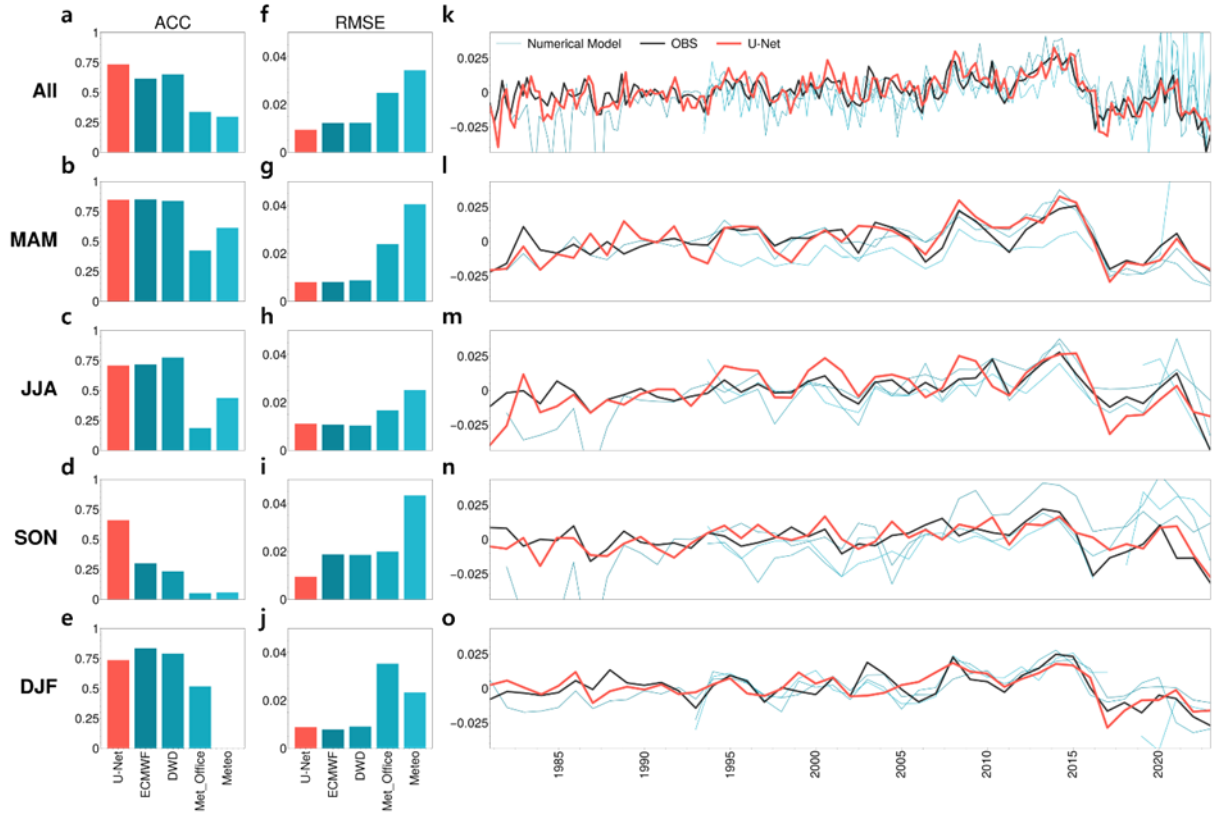

Figure 2: Seasonal performance of U-Net and numerical models in terms of ACC, RMSE, and time series. Panels (a–e) show the ACC of U-Net (red bars) and numerical models (blue bars; ECMWF, DWD, Met Office, Météo-France) for all seasons, autumn, winter, spring, and summer, respectively. Panels (f–j) show the RMSE of U-Net (red bars) and the numerical models (blue bars) for the same seasonal divisions. Panels (k–o) show the time series of sea ice concentration (SIC) predicted by U-Net (red lines) and the numerical models (blue lines), together with observations (black lines) for all seasons and for each individual season.

3.2 Spatial-temporal contribution of predictive variables

After evaluating the Antarctic as a whole, we further examined prediction skill across five sectors. During autumn (MAM), when sea ice expands, most regions exhibit relatively high skill, except for the AB sector (Fig. 3e). The Weddell sector in particular exhibits strong predictability in austral autumn (MAM), consistent with results from numerical models such as ECMWF (Fig. S3b). In the austral spring (SON), numerical models generally display low predictive performance. By contrast, U-Net maintains consistently high skill, achieving ACC values of 0.77 in the Indian sector and 0.85 in the Ross sector. These values far exceed those of the best numerical model (Met Office), which reached only 0.42 and 0.40, respectively (Fig. S3d). Taken together, the U-Net outperforms numerical models not only in overall Antarctic predictions but also in regional sea ice variability, most notably in the Indian and Ross sectors.

https://doi.org/10.5194/egusphere-2026-1556
Preprint. Discussion started: 5 June 2026

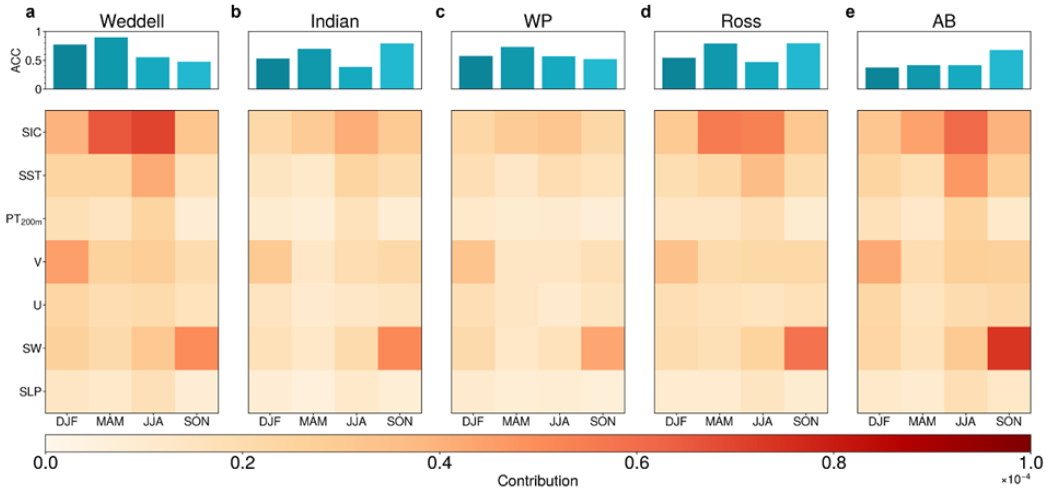

Figure 3: Regional and seasonal analysis of RMSD and U-Net performance. Panels (a-e) show ACC and RMSD in the Weddell, Indian, West Pacific (WP), Ross and Amundsen-Bellingshausen (AB) region, respectively.

To identify which variables contribute to the predictive skill of the SIC with a one-season lead, the Root-Mean-Squared Difference (RMSD) was calculated by zeroing individual input variables across different regions and seasons (Fig. 3). It is clear that the previous-season SICs contribute significantly to the prediction skill during autumn and winter, coinciding with strong persistence of sea ice anomalies, indicating high autocorrelation (Fig. S4). Regionally, the highest SIC contributions appear in Weddell and adjacent Southwest Antarctic regions (Ross, AB). Conversely, SIC contributions are smaller in Eastern Antarctic regions (Indian, WP) with weaker seasonal variability. The one-season lagged correlation of SIC, when separated by season for the West (Weddell, Ross, AB) and East (Indian, WP) Antarctic sectors, reveals a distinct difference between the two regions. In the West Antarctic, the seasonal autocorrelations are relatively high, with values of 0.77 in autumn and 0.68 in winter. In contrast, the East Antarctic shows lower correlations, with values of 0.59 in autumn and 0.50 in winter (Fig. S4). In West Antarctica, sea ice exhibits stronger temporal persistence compared to East Antarctica, and this property is well reflected in the U-Net model.

SST contributions are similar to SIC patterns, displaying higher RMSD values during winter, but substantially lower values in autumn, indicating different seasonal sensitivity. SST is particularly influential in the Weddell, Ross, and AB regions, where strong ocean–sea ice coupling driven by gyre dynamics and Circumpolar Deep Water intrusions amplifies the effect of ocean heat anomalies on sea ice variability (Dinniman et al., 2011; Holland and Kwok, 2012; Wang et al., 2024). Furthermore, large-scale circulation features such as the Amundsen Sea Low (ASL) enhance this sensitivity through atmosphere–ocean–ice feedbacks, while the Indian and WP regions, located farther from the ASL in West Antarctica, experience comparatively weaker influences. In contrast, during summer (DJF) and spring (SON), the other variables emerge as important predictors. V wind is highly influential in summer, significantly affecting sea ice variability. SW shows high RMSD values in spring across all regions, peaking notably in the AB region. Despite the lower prediction skill in AB during

https://doi.org/10.5194/egusphere-2026-1556
Preprint. Discussion started: 5 June 2026

the other seasons (Fig. 3e), predictions for spring SIC exhibit relatively higher skill aligned with elevated SW contributions. Therefore, summer V wind and spring SW, particularly in the AB region, warrant further detailed investigation.

3.3 Physical interpretation of key predictors

3.3.1 Role of Meridional wind

Deep learning not only enhances predictive skill but also advances the understanding of underlying physical processes. By quantifying the contributions of different variables, deep learning models can shed light on the mechanisms that drive sea ice variability. A positive signed-contribution indicates that anomalous southerly wind is related to positive sea ice anomaly in the following season, whereas a negative signed-contribution indicates a negative sea ice anomaly. Given its large contribution in summer, we investigated whether the V wind promotes sea ice growth or decline. The SC maps for V wind show clear seasonal contrasts. In summer, strong negative contributions occur at high latitudes in the AB region, particularly near the climatological sea-ice edge (Fig. 4a). When the high-contribution area (73°–78°S, 230°–270°E) was set to zero anomalies and compared to the original, the negative signed-contribution remained robust (Fig. 4c; r = −0.68, significant at the 99% level). This suggests that enhanced southerly winds promote summer sea ice loss by driving ice northward, thinning the ice, and fostering polynya formation, which inhibits new ice growth (Song et al., 2025). Consistently, negative V-wind contributions dominate only in summer (Fig. S5), highlighting their key role in summer sea-ice variability.

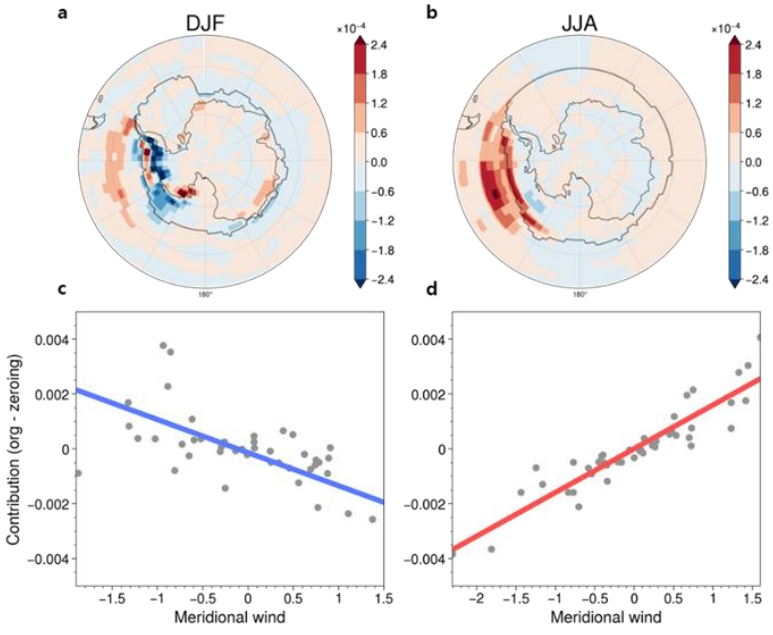

Figure 4: Signed-contribution (SC) maps in summer and winter. Panel (a) shows the SC map for meridional wind (V) over the AB region during DJF (December–January–February), and panel (b) shows the corresponding map during JJA (June–July–August). Panels (c) and (d) display the corresponding V fields overlaid with SIC differences for DJF and JJA, respectively.

https://doi.org/10.5194/egusphere-2026-1556
Preprint. Discussion started: 5 June 2026

In contrast, winter exhibits strong positive V wind contributions outside the sea ice edge, suggesting that the southerly wind anomalies lead to increased sea ice (Fig. 4b). To verify this relationship, the region with strong contributions (68°–73°S, 230°–270°E) was replaced with its climatological values and compared with the original prediction. Even after the replacement, the positive signed-contribution remained robust (Fig. 4d; r = 0.92), significant at the 99% confidence level. The sea ice transported equatorward in winter, together with the intrusion of cold polar air into northern regions, tends to persist longer under colder conditions, further enhancing overall extent (Song et al., 2025). In addition, southerly winds drive the formation of polynyas, providing favorable conditions for new ice formation during winter. This positive relationship has been consistently demonstrated in previous studies (Holland and Kwok, 2012; Stammerjohn et al., 2003; Turner et al., 2016; Wagner et al., 2021). Thus, winter sea ice exhibits a strong positive correlation with V wind (r = 0.92), which is significant at the 99% confidence level.

In addition to the AB region, other regions also exhibit a clear seasonal contrast: during summer, V wind generally makes a negative signed-contribution to sea ice, while in the other seasons its signed-contribution is positive (Fig. S5). This seasonal pattern is consistent with the tendencies described earlier. In most cases, the spatial distribution of V wind contributions closely matches the regions where sea ice is predicted. An exception occurs in the Weddell region, where the negative summer signed-contribution does not remain confined locally but instead extends eastward toward East Antarctica (Fig. S5a). This suggests that, in the Weddell region, the influence of V wind covers a broader area compared to the other regions.

These spatial and seasonal contrasts can be interpreted in the context of large-scale circulation, particularly the Amundsen Sea Low (ASL), which modulates meridional wind patterns and Antarctic sea ice variability (Holland et al., 2018). Seasonal changes in the ASL strength and position alter southerly flow over the Ross and AB Seas (Stammerjohn et al., 2015), enhancing winter sea ice through cold-air advection and coastal expansion while promoting summer sea ice loss via northward ice advection and reduced ice formation (Holland et al., 2018; Raphael et al., 2019). A deepened ASL in spring can further precondition negative summer anomalies by strengthening meridional transport (Holland et al., 2018), consistent with the summer V wind contributions (Fig. 4a,c).

3.3.2 Role of Shortwave radiation

As shown in Fig. 3e, a strong contribution of the SW to AB sea ice is found during spring, suggesting that the preceding winter SW plays a critical role in sea ice changes during the following spring. To examine this process in detail, Fig. 5 shows the signed-contribution of SW for AB sea ice during spring. Notably, there are contrasting contributions of the SW to the sea ice, as shown in Fig. 5a. The SW exhibits contrasting effects with latitude: negative contributions at lower latitudes and positive contributions at higher latitudes. Higher SW increases surface energy input and accelerates sea ice melting, leading to reduced sea ice. In contrast to the negative relationships in the lower latitudes, the positive associations at higher latitudes

https://doi.org/10.5194/egusphere-2026-1556
Preprint. Discussion started: 5 June 2026

require further interpretation. Although SW radiation is minimal during winter at high latitudes, it can still convey information indirectly through longwave cloud feedbacks.

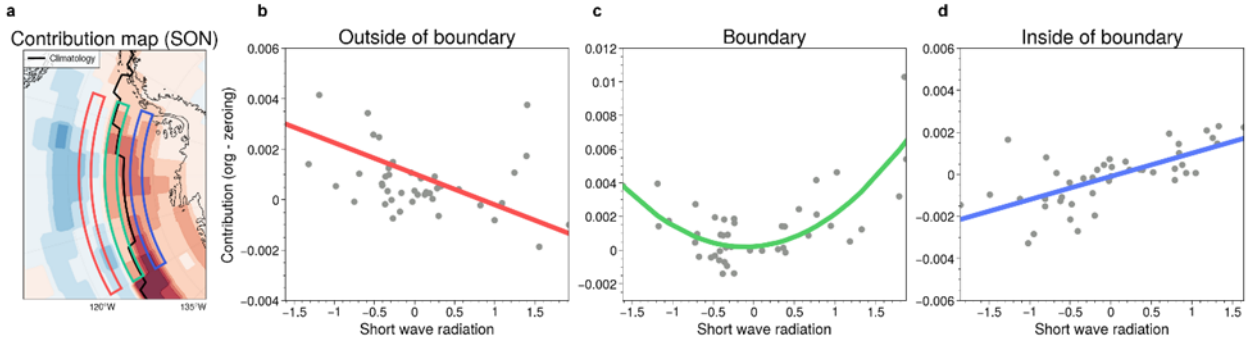

Figure 5: Contribution of downward shortwave radiation (SW) in three subregions of the AB region. Panel (a) shows the signed-contribution map of SW during SON (September–October–November) along with the classification of three subregions based on proximity to the sea ice edge: outside of boundary (red), boundary (green), and inside of boundary (blue). Panels (b-d) show the SW and SIC differences for the outside, boundary, and inside regions, respectively.

To examine the latitude-dependent transition near 65°S, we analyzed three latitude bands (outer: 61.5°S–62.5°S, boundary: 64.5°S–65.5°S, inner: 67.5°S–68.5°S). The outer band shows a clear negative relationship, indicating that increased SW promotes sea ice loss through enhanced absorption over open water and sparse ice, consistent with the ice–albedo feedback (Goosse et al., 2018; Kashiwase et al., 2017). The contribution maps further support SW as a key driver of spring sea ice variability.

However, in the inner region where sea ice persists, the surface albedo remains high, limiting SW-driven warming, especially during winter when SW is minimal. This weakens the negative SW–sea ice relationship observed in the outer region and instead yields a positive correlation (Fig. 5d). In winter, SW anomalies are negatively correlated with cloud cover (Fig. S6a), implying that cloud-related longwave forcing becomes the dominant warming mechanism (Fig. S6b, Moon & Wettlaufer, 2011), which reduces sea ice extent (Fig. S6c). Although longwave radiation is not explicitly included in the model, its influence can be implicitly captured through SW as a proxy for cloud variability.

Interestingly, the boundary region exhibits nonlinear behavior, with negative slopes for SW < 0 and positive slopes for SW > 0 (Fig. 5c). This region features strong SIC variability and mixed surface conditions, where both open ocean and ice-covered areas coexist. Under reduced SW, the response resembles that of the outer region, where SW promotes sea ice melt. In contrast, high SW conditions likely correspond to periods with abundant sea ice and reduced cloud cover, yielding a positive slope similar to the inner region. This regime-dependent behavior highlights a transitional zone where deep learning can capture nonlinear responses that linear methods may miss. Consistently, the model reproduces clear spatial boundaries and coherent seasonal patterns across all sectors (Fig. S7).

In the AB region, the contribution of SW during SON is particularly pronounced as multiple processes act in concert. The seasonal transition in this sector is marked by thin and unstable sea ice (Wang et al., 2020), which makes the ice cover highly

https://doi.org/10.5194/egusphere-2026-1556
Preprint. Discussion started: 5 June 2026

responsive to relatively small changes in radiative forcing. This sensitivity is further amplified by the ASL, which is situated over West Antarctica including the AB region, and whose influence on cloud variability modulates SW reaching the surface and intensifies the ice–radiation feedback. At the same time, large-scale teleconnections such as ENSO and the Southern Annular Mode shape atmospheric circulation and cloud distributions, providing additional modulation of SW forcing. Because these teleconnections exert particularly strong impacts on the AB sector (Clem et al., 2017; Yiu and Maycock, 2019), the combined influences reinforce each other, generating a nonlinear response of sea ice to SW that is most prominent in this region during SON.

4 Discussion and conclusion

Leveraging a multi-century LENS2 dataset, our deep learning framework achieved skillful prediction of Antarctic sea ice variability. The approach offers clear advantages over traditional methods: once trained, the model can generate predictions with substantially reduced computational cost while effectively learning nonlinear and high-dimensional relationships among atmosphere, ocean, and sea ice. These strengths enabled the model to capture both large-scale patterns and regional variability, with particularly strong performance in representing the pronounced variability of summer sea ice—one of the most challenging aspects for numerical models. These results underscore the promise of deep learning not only in improving predictive skill but also in complementing physics-based dynamical frameworks in climate research.

Equally important, the framework proved useful for understanding the mechanisms driving variability. Instead of offering only black-box predictions, the model outputs and attribution analysis revealed distinct seasonal and spatial characteristics. For instance, V winds were found to play differing roles depending on the season, while SW exhibited opposite-signed contributions across latitudes, reflecting not only direct radiative effects but also co-varying cloud-related processes that shape the early-spring surface energy balance. SW therefore exerted heterogeneous impacts across regions, implicitly linking to cloud-related processes. Moreover, the behavior of the AB sector relative to the climatological sea ice edge illustrated how the model can shed light on the spatial structure of variability. These insights demonstrate that the approach is not limited to prediction but can also provide interpretable perspectives on Antarctic sea ice dynamics.

Despite these advances, several opportunities for further improvement remain. Our model primarily captures intra-seasonal influences, but abrupt sea ice changes may also be driven by episodic or compounded external forcings that are not fully represented by preceding-season conditions. Expanding the spatiotemporal domain could therefore improve the prediction of extreme events. In addition, sector-based partitioning may introduce artificial boundaries and obscure cross-regional dynamics near sector edges. Extending the framework toward spatially explicit prediction would enable more detailed mechanistic assessments, although it would increase model complexity and require careful attention to interpretability.

The analysis of variable contributions further underscores this point. For instance, the summer V wind exhibited locally opposing impacts even within adjacent areas, suggesting that while large-scale relationships are well captured, local

https://doi.org/10.5194/egusphere-2026-1556
Preprint. Discussion started: 5 June 2026

consistency can be further improved. Moreover, the choice of input variables directly influences the explanatory power of the model. In the current design, SW implicitly substitutes for cloud influences, reflecting the model's ability to infer missing processes through proxy variables. Nonetheless, incorporating explicit cloud properties or other physically direct predictors would enable clearer attribution and deeper insight into the coupled atmosphere–ocean–sea ice system. At present, the model is primarily trained with information confined to the polar region. However, Antarctic sea ice is strongly influenced, both directly and indirectly, by atmospheric and oceanic variability originating from the tropics (Nuncio and Yuan, 2015; Purich et al., 2016). Future work should extend the spatial domain to include low-latitude forcings such as ENSO, allowing a more comprehensive representation of the coupled system.

https://doi.org/10.5194/egusphere-2026-1556
Preprint. Discussion started: 5 June 2026

Code availability

The code used in this study is being prepared for public release and will be deposited in a GitHub repository upon final publication of the manuscript. An archived release with a DOI will also be provided. Until public release, access to the code is available from the corresponding author upon reasonable request.

Data availability

The datasets for training and test are available from the corresponding author on reasonable request. The NCEP/DOE reanalysis data were downloaded from https://gdex.ucar.edu/datasets/d651055/ and https://www.psl.noaa.gov/data/gridded/data.ncep.reanalysis2.html. The ORAS5 reanalysis data were downloaded from https://cds.climate.copernicus.eu/datasets/reanalysis-oras5?tab=overview. NSIDC's Nimbus-7 SMMR and DMSP SSM/I-SSMIS Passive Microwave Data, Version 2 were downloaded from https://nsidc.org/data/nsidc-0051/versions/2.

Author contributions

G. Baek compiled and preprocessed the data, trained the deep-learning model, conducted the analyses, prepared the figures, and wrote the manuscript. J. Ko contributed to the design and implementation of the deep-learning architecture and provided support during the model training process. E.K. Jin reviewed the results and provided scientific guidance based on domain expertise. J.-S. Kug designed the research, provided guidance throughout the overall study, discussed the results, and reviewed the manuscript.

Competing interests

The authors declare there are no conflicts of interest for this manuscript.

Acknowledgements

We acknowledge support from the Korea Institute of Marine Science & Technology Promotion (KIMST), funded by the Ministry of Oceans and Fisheries.

Financial support

This research was supported by Korea Institute of Marine Science & Technology Promotion (KIMST) funded by the Ministry of Oceans and Fisheries (RS-2025-02219198).

https://doi.org/10.5194/egusphere-2026-1556
Preprint. Discussion started: 5 June 2026

References

Barnes, E. A., Toms, B., Hurrell, J. W., Ebert-Uphoff, I., Anderson, C., and Anderson, D.: Indicator Patterns of Forced Change Learned by an Artificial Neural Network, Journal of Advances in Modeling Earth Systems, 12, e2020MS002195, https://doi.org/10.1029/2020MS002195, 2020.

Bushuk, M., Winton, M., Haumann, F. A., Delworth, T., Lu, F., Zhang, Y., Jia, L., Zhang, L., Cooke, W., Harrison, M., Hurlin, B., Johnson, N. C., Kapnick, S. B., McHugh, C., Murakami, H., Rosati, A., Tseng, K.-C., Wittenberg, A. T., Yang, X., and Zeng, F.: Seasonal Prediction and Predictability of Regional Antarctic Sea Ice, https://doi.org/10.1175/JCLI-D-20-0965.1, 2021.

Cai, S., Hsu, P.-C., and Liu, F.: Changes in polar amplification in response to increasing warming in CMIP6, Atmospheric and Oceanic Science Letters, 14, 100043, https://doi.org/10.1016/j.aosl.2021.100043, 2021.

Chen, D. and Yuan, X.: A Markov Model for Seasonal Forecast of Antarctic Sea Ice, 2004.

Cheon, M., Choi, Y.-H., Kang, S.-Y., Choi, Y., Lee, J.-G., and Kang, D.: KARINA: An Efficient Deep Learning Model for Global Weather Forecast, https://doi.org/10.48550/arXiv.2403.10555, 13 March 2024.

Clem, K. R., Renwick, J. A., and McGregor, J.: Large-Scale Forcing of the Amundsen Sea Low and Its Influence on Sea Ice and West Antarctic Temperature, https://doi.org/10.1175/JCLI-D-16-0891.1, 2017.

Comiso, J. C., Gersten, R. A., Stock, L. V., Turner, J., Perez, G. J., and Cho, K.: Positive Trend in the Antarctic Sea Ice Cover and Associated Changes in Surface Temperature, Journal of Climate, 30, 2251–2267, https://doi.org/10.1175/JCLI-D-16-0408.1, 2017.

Copernicus Climate Change Service and Climate Data Store: Seasonal forecast monthly statistics on single levels, https://doi.org/10.24381/cds.68dd14c3, 2018.

Copernicus Climate Change Service and Climate Data Store: ORAS5 global ocean reanalysis monthly data from 1958 to present, https://doi.org/https://doi.org/10.24381/cds.67e8eeb7, 2021.

Curry, J. A., Schramm, J. L., and Ebert, E. E.: Sea Ice-Albedo Climate Feedback Mechanism, 1995.

Danabasoglu, G., Lamarque, J.-F., Bacmeister, J., Bailey, D. A., DuVivier, A. K., Edwards, J., Emmons, L. K., Fasullo, J., Garcia, R., Gettelman, A., Hannay, C., Holland, M. M., Large, W. G., Lauritzen, P. H., Lawrence, D. M., Lenaerts, J. T. M., Lindsay, K., Lipscomb, W. H., Mills, M. J., Neale, R., Oleson, K. W., Otto-Bliesner, B., Phillips, A. S., Sacks, W., Tilmes, S., van Kampenhout, L., Vertenstein, M., Bertini, A., Dennis, J., Deser, C., Fischer, C., Fox-Kemper, B., Kay, J. E., Kinnison, D., Kushner, P. J., Larson, V. E., Long, M. C., Mickelson, S., Moore, J. K., Nienhouse, E., Polvani, L., Rasch, P. J., and Strand, W. G.: The Community Earth System Model Version 2 (CESM2), Journal of Advances in Modeling Earth Systems, 12, e2019MS001916, https://doi.org/10.1029/2019MS001916, 2020.

DiGirolamo, N., Parkinson, C., Cavalieri, D., Gloersen, P., and Zwally, H.: Sea Ice Concentrations from Nimbus-7 SMMR and DMSP SSM/I-SSMIS Passive Microwave Data, Version 2, https://doi.org/10.5067/MPYG15WAA4WX, 2022.

https://doi.org/10.5194/egusphere-2026-1556
Preprint. Discussion started: 5 June 2026

Dinniman, M. S., Klinck, J. M., and Smith, W. O.: A model study of Circumpolar Deep Water on the West Antarctic Peninsula and Ross Sea continental shelves, Deep Sea Research Part II: Topical Studies in Oceanography, 58, 1508–1523, https://doi.org/10.1016/j.dsr2.2010.11.013, 2011.

Doddridge, E. W., Hobbs, W. R., Auger, M., Boyd, P. W., Chua, S. M. T., Cook, S., Corney, S., Emmerson, L., Fraser, A. D., Heil, P., Kelly, N., Lannuzel, D., Li, X., Liniger, G., Massom, R. A., Meyer, A., Reid, P., Southwell, C., Spence, P., Steketee, A., Swadling, K. M., Teder, N., Wienecke, B., Wongpan, P., and Yamazaki, K.: Impacts of Antarctic summer sea-ice extremes, PNAS Nexus, 4, pgaf164, https://doi.org/10.1093/pnasnexus/pgaf164, 2025.

Fogt, R. L., Sleinkofer, A. M., Raphael, M. N., and Handcock, M. S.: A regime shift in seasonal total Antarctic sea ice extent in the twentieth century, Nat. Clim. Chang., 12, 54–62, https://doi.org/10.1038/s41558-021-01254-9, 2022.

Goosse, H., Kay, J. E., Armour, K. C., Bodas-Salcedo, A., Chepfer, H., Docquier, D., Jonko, A., Kushner, P. J., Lecomte, O., Massonnet, F., Park, H.-S., Pithan, F., Svensson, G., and Vancoppenolle, M.: Quantifying climate feedbacks in polar regions, Nat Commun, 9, 1919, https://doi.org/10.1038/s41467-018-04173-0, 2018.

He, K., Zhang, X., Ren, S., and Sun, J.: Delving Deep into Rectifiers: Surpassing Human-Level Performance on ImageNet Classification, in: 2015 IEEE International Conference on Computer Vision (ICCV), 2015 IEEE International Conference on Computer Vision (ICCV), 1026–1034, https://doi.org/10.1109/ICCV.2015.123, 2015.

Hogg, J., Fonoberova, M., and Mezić, I.: Exponentially decaying modes and long-term prediction of sea ice concentration using Koopman mode decomposition, Sci Rep, 10, 16313, https://doi.org/10.1038/s41598-020-73211-z, 2020.

Holland, M. M., Landrum, L., Raphael, M. N., and Kwok, R.: The Regional, Seasonal, and Lagged Influence of the Amundsen Sea Low on Antarctic Sea Ice, Geophysical Research Letters, 45, 11,227-11,234, https://doi.org/10.1029/2018GL080140, 2018.

Holland, P. R. and Kwok, R.: Wind-driven trends in Antarctic sea-ice drift, Nature Geosci, 5, 872–875, https://doi.org/10.1038/ngeo1627, 2012.

Huang, B., Thorne, P. W., Banzon, V. F., Boyer, T., Chepurin, G., Lawrimore, J. H., Menne, M. J., Smith, T. M., Vose, R. S., and Zhang, H.-M.: Extended Reconstructed Sea Surface Temperature, Version 5 (ERSSTv5): Upgrades, Validations, and Intercomparisons, https://doi.org/10.1175/JCLI-D-16-0836.1, 2017.

Ioffe, S. and Szegedy, C.: Batch Normalization: Accelerating Deep Network Training by Reducing Internal Covariate Shift, https://doi.org/10.48550/arXiv.1502.03167, 2 March 2015.

Kanamitsu, M., Ebisuzaki, W., Woollen, J., Yang, S.-K., Hnilo, J. J., Fiorino, M., and Potter, G. L.: NCEP–DOE AMIP-II Reanalysis (R-2), https://doi.org/10.1175/BAMS-83-11-1631, 2002.

Kashiwase, H., Ohshima, K. I., Nihashi, S., and Eicken, H.: Evidence for ice-ocean albedo feedback in the Arctic Ocean shifting to a seasonal ice zone, Sci Rep, 7, 8170, https://doi.org/10.1038/s41598-017-08467-z, 2017.

Li, G., Cheng, L., Zhu, J., Trenberth, K. E., Mann, M. E., and Abraham, J. P.: Increasing ocean stratification over the past half-century, Nat. Clim. Chang., 10, 1116–1123, https://doi.org/10.1038/s41558-020-00918-2, 2020.

https://doi.org/10.5194/egusphere-2026-1556
Preprint. Discussion started: 5 June 2026

Lucas, N. S., Brearley, J. A., Hendry, K. R., Spira, T., Braakmann-Folgmann, A., Abrahamsen, E. P., Meredith, M. P., and Tarling, G. A.: Giant iceberg meltwater increases upper-ocean stratification and vertical mixing, Nat. Geosci., 18, 305–312, https://doi.org/10.1038/s41561-025-01659-7, 2025.

Massom, R. A., Scambos, T. A., Bennetts, L. G., Reid, P., Squire, V. A., and Stammerjohn, S. E.: Antarctic ice shelf disintegration triggered by sea ice loss and ocean swell, Nature, 558, 383–389, https://doi.org/10.1038/s41586-018-0212-1, 2018.

Massonnet, F., Barreira, S., Barthélemy, A., Bilbao, R., Blanchard-Wrigglesworth, E., Blockley, E., Bromwich, D. H., Bushuk, M., Dong, X., Goessling, H. F., Hobbs, W., Iovino, D., Lee, W.-S., Li, C., Meier, W. N., Merryfield, W. J., Moreno-Chamarro, E., Morioka, Y., Li, X., Niraula, B., Petty, A., Sanna, A., Scilingo, M., Shu, Q., Sigmond, M., Sun, N., Tietsche, S., Wu, X., Yang, Q., and Yuan, X.: SIPN South: six years of coordinated seasonal Antarctic sea ice predictions, Front. Mar. Sci., 10, https://doi.org/10.3389/fmars.2023.1148899, 2023.

Morioka, Y., Doi, T., Iovino, D., Masina, S., and Behera, S. K.: Role of sea-ice initialization in climate predictability over the Weddell Sea, Sci Rep, 9, 2457, https://doi.org/10.1038/s41598-019-39421-w, 2019.

Nair, V. and Hinton, G. E.: Rectified Linear Units Improve Restricted Boltzmann Machines, 2010.

Nuncio, M. and Yuan, X.: The Influence of the Indian Ocean Dipole on Antarctic Sea Ice, https://doi.org/10.1175/JCLI-D-14-00390.1, 2015.

Parkinson, C. L. and Cavalieri, D. J.: Antarctic sea ice variability and trends, 1979–2010, The Cryosphere, 6, 871–880, https://doi.org/10.5194/tc-6-871-2012, 2012.

Purich, A. and Doddridge, E. W.: Record low Antarctic sea ice coverage indicates a new sea ice state, Commun Earth Environ, 4, 314, https://doi.org/10.1038/s43247-023-00961-9, 2023.

Purich, A., England, M. H., Cai, W., Chikamoto, Y., Timmermann, A., Fyfe, J. C., Frankcombe, L., Meehl, G. A., and Arblaster, J. M.: Tropical Pacific SST Drivers of Recent Antarctic Sea Ice Trends, https://doi.org/10.1175/JCLI-D-16-0440.1, 2016.

Raphael, M. N., Holland, M. M., Landrum, L., and Hobbs, W. R.: Links between the Amundsen Sea Low and sea ice in the Ross Sea: seasonal and interannual relationships, Clim Dyn, 52, 2333–2349, https://doi.org/10.1007/s00382-018-4258-4, 2019.

Rodgers, K. B., Lee, S.-S., Rosenbloom, N., Timmermann, A., Danabasoglu, G., Deser, C., Edwards, J., Kim, J.-E., Simpson, I. R., Stein, K., Stuecker, M. F., Yamaguchi, R., Bódai, T., Chung, E.-S., Huang, L., Kim, W. M., Lamarque, J.-F., Lombardozzi, D. L., Wieder, W. R., and Yeager, S. G.: Ubiquity of human-induced changes in climate variability, Earth System Dynamics, 12, 1393–1411, https://doi.org/10.5194/esd-12-1393-2021, 2021.

Ronneberger, O., Fischer, P., and Brox, T.: U-Net: Convolutional Networks for Biomedical Image Segmentation, in: Medical Image Computing and Computer-Assisted Intervention – MICCAI 2015, 234–241, https://doi.org/10.1007/978-3-319-24574-4_28, 2015.

https://doi.org/10.5194/egusphere-2026-1556
Preprint. Discussion started: 5 June 2026

Shin, N.-Y., Ham, Y.-G., Kim, J.-H., Cho, M., and Kug, J.-S.: Application of Deep Learning to Understanding ENSO Dynamics, https://doi.org/10.1175/AIES-D-21-0011.1, 2022.

Shin, N.-Y., Kim, D., Kang, D., Kim, H., and Kug, J.-S.: Deep learning reveals moisture as the primary predictability source of MJO, npj Clim Atmos Sci, 7, 11, https://doi.org/10.1038/s41612-023-00561-6, 2024.

Song, H., Choi, Y., Doddridge, E. W., and Marshall, J.: The Responses of Antarctic Sea Ice and Overturning Cells to Meridional Wind Forcing, https://doi.org/10.1175/JCLI-D-24-0070.1, 2025.

Stammerjohn, S. E., Drinkwater, M. R., Smith, R. C., and Liu, X.: Ice-atmosphere interactions during sea-ice advance and retreat in the western Antarctic Peninsula region, Journal of Geophysical Research: Oceans, 108, https://doi.org/10.1029/2002JC001543, 2003.

Stammerjohn, S. E., Maksym, T., Massom, R. A., Lowry, K. E., Arrigo, K. R., Yuan, X., Raphael, M., Randall-Goodwin, E., Sherrell, R. M., and Yager, P. L.: Seasonal sea ice changes in the Amundsen Sea, Antarctica, over the period of 1979–2014, Elementa: Science of the Anthropocene, 3, 000055, https://doi.org/10.12952/journal.elementa.000055, 2015.

Turner, J., Hosking, J. S., Marshall, G. J., Phillips, T., and Bracegirdle, T. J.: Antarctic sea ice increase consistent with intrinsic variability of the Amundsen Sea Low, Clim Dyn, 46, 2391–2402, https://doi.org/10.1007/s00382-015-2708-9, 2016.

Venegas, R. M., Acevedo, J., and Treml, E. A.: Three decades of ocean warming impacts on marine ecosystems: A review and perspective, Deep Sea Research Part II: Topical Studies in Oceanography, 212, 105318, https://doi.org/10.1016/j.dsr2.2023.105318, 2023.

Wagner, T. J. W., Eisenman, I., and Mason, H. C.: How Sea Ice Drift Influences Sea Ice Area and Volume, Geophysical Research Letters, 48, e2021GL093069, https://doi.org/10.1029/2021GL093069, 2021.

Wang, J., Massonnet, F., Goosse, H., Luo, H., Barthélemy, A., and Yang, Q.: Synergistic atmosphere-ocean-ice influences have driven the 2023 all-time Antarctic sea-ice record low, Commun Earth Environ, 5, 415, https://doi.org/10.1038/s43247-024-01523-3, 2024.

Wang, X., Jiang, W., Xie, H., Ackley, S., and Li, H.: Decadal Variations of Sea Ice Thickness in the Amundsen-Bellingshausen and Weddell Seas Retrieved From ICESat and IceBridge Laser Altimetry, 2003–2017, Journal of Geophysical Research: Oceans, 125, e2020JC016077, https://doi.org/10.1029/2020JC016077, 2020.

Wang, Y., Yuan, X., Ren, Y., Bushuk, M., Shu, Q., Li, C., and Li, X.: Subseasonal Prediction of Regional Antarctic Sea Ice by a Deep Learning Model, Geophysical Research Letters, 50, e2023GL104347, https://doi.org/10.1029/2023GL104347, 2023.

Yang, Z., Liu, J., Song, M., Hu, Y., Yang, Q., Fan, K., Graversen, R. G., and Zhou, L.: Extended seasonal prediction of Antarctic sea ice concentration using ANTSIC-UNet, The Cryosphere, 19, 6381–6402, https://doi.org/10.5194/tc-19-6381-2025, 2025.

Yiu, Y. Y. S. and Maycock, A. C.: On the Seasonality of the El Niño Teleconnection to the Amundsen Sea Region, https://doi.org/10.1175/JCLI-D-18-0813.1, 2019.

https://doi.org/10.5194/egusphere-2026-1556
Preprint. Discussion started: 5 June 2026

Yu, F. and Koltun, V.: Multi-Scale Context Aggregation by Dilated Convolutions, https://doi.org/10.48550/arXiv.1511.07122, 30 April 2016.

Zampieri, L., Goessling, H. F., and Jung, T.: Predictability of Antarctic Sea Ice Edge on Subseasonal Time Scales, Geophysical Research Letters, 46, 9719–9727, https://doi.org/10.1029/2019GL084096, 2019.

Zeiler, M. D. and Fergus, R.: Visualizing and Understanding Convolutional Networks, in: Computer Vision – ECCV 2014, 818–833, https://doi.org/10.1007/978-3-319-10590-1_53, 2014.

Zhang, L., Delworth, T. L., Yang, X., Zeng, F., Lu, F., Morioka, Y., and Bushuk, M.: The relative role of the subsurface Southern Ocean in driving negative Antarctic Sea ice extent anomalies in 2016–2021, Commun Earth Environ, 3, 302, https://doi.org/10.1038/s43247-022-00624-1, 2022.